OPTIMISATION OF MILLING OPERATION ON GRAPHENE OXIDE-EPOXY NANOCOMPOSITE BY TAGUCHI METHOD

A Major Project report submitted in partial fulfillment for the award of the Degree of

MASTER OF TECHNOLOGY

IN

POLYMER TECHNOLOGY

Submitted by

VIVEK NIRWAL
2K15/PTE/14

UNDER THE ESTEEMED GUIDANCE OF

PROF. D. KUMAR and DR. JAY SINGH

Department of Applied Chemistry & Polymer Technology

Delhi Technological University, Delhi-110042

July 2017

CERTIFICATE

This is to certify that the project report entitled **"Optimization Of Milling Operation On Graphene Oxide-Epoxy Nanocomposite By Taguchi Method"** submitted by **Vivek Nirwal (2K15/PTE/14)** in partial fulfillment for the award of degree of Master of Technology in Polymer Technology to Delhi Technological University, Delhi, is a record of the work carried out by him under our supervision. The project embodies the original work carried out by him has not been submitted to any other degree of this or any other university to the best of our knowledge.

Prof. D. Kumar
Professor
Department of Applied Chemistry
& Polymer Technology
Delhi Technological University
New Delhi -110042

Dr. Jay Singh
Department of Applied Chemistry
& Polymer Technology
Delhi Technological University
New Delhi -110042

Dr. Archna Rani
Head of the department
Department of Applied Chemistry & Polymer Technology
Delhi Technological University
New Delhi -110042

DECLARATION

I **VIVEK NIRWAL** hereby declare that the thesis entitled **"Optimisation Of Milling Operation On Graphene Oxide-Epoxy Nanocomposite By Taguchi Method"** is an authentic record of research work done by me under the supervision of **Prof. D. Kumar,** Professor, and **Dr. Jay Singh**, Delhi Technological University. This work has not been previously submitted for the award of any degree or diploma of this or any other University/Institute. The matter embodied in this project report is original and not copied from any source without proper citation.

Dated VIVEK NIRWAL

ACKNOWLEDGEMENT

It gives me immense pleasure to express my deepest sense of gratitude and sincere thanks to highly respected and esteemed guide **Prof. D. Kumar & Dr. Jay Singh**, for their valuable guidance, encouragement and help for completing this work. Their useful suggestions for this whole work and co-operative behavior are sincerely acknowledged.

I also wish to express my gratitude to **Dr. Archna Rani**, HOD (Department of Applied Chemistry & Polymer Technology) for her kind hearted support. I am also grateful to all teachers for their constant support and guidance.

I'm grateful to **Dr. Ranganath Sangri & Mr. Sunil** for his invaluable guidance, support and motivation in my research work.

I also wish to express my indebtedness to my parents as well as my family members whose blessings and support always helped me to face the challenges ahead.

At the end I would like to express my sincere thanks to all my friends and others who helped me directly or indirectly during this project work.

VIVEK NIRWAL

LIST OF FIGURES

LIST OF TABLES

CONTENTS

ABSTRACT

This project introduces the application of Taguchi optimization methodology in optimizing the cutting parameters of end-milling process for machining the Graphene Oxide reinforced epoxy hybrid composite material under dry condition. The machining parameters which are chosen to be evaluated in this study are the depth of cut (d), cutting speed (S) and feed rate (f). While, the response factors to be measured are the surface roughness of the machined composite surface and the cutting force. An orthogonal array of the Taguchi method was set-up and used to analyze the effect of the milling parameters on the surface roughness, material removal rate and cutting force. The result from this study shows that the application of the Taguchi method can determine the best combination of machining parameters that can provide the optimal machining response conditions which are the lowest surface roughness and lowest cutting force value. For the best surface finish, A1–B3–C3 (d = 0.4 mm, S = 1500 rpm, f = 60 mm/min) is found to be the optimized combination of levels for all the three control factors from the analysis. Meanwhile, the optimized combination of levels for all the three control factors from the analysis which provides the lowest cutting force was found to be A2–B2–C2 (d = 0.6 mm, S = 1000 rpm, f = 40 mm/min).

CHAPTER 1

INTRODUCTION

Graphene is single layer of pure carbon ; it is tightly packed layer of carbon atoms which is bonded together in a hexagonal lattice like a honeycomb. In other words it is an allotrope of carbon in the structure of a plane of sp^2 bonded atoms having bond length of 0.142 nm. Layers of graphene stacked on each other on the top form graphite. These layers have interplanar spacing of 0.335 nm[2].

Low density composites and high strength base are for the most preferable for various applications in the world. Unique properties such as high rigidity and specific strength, high mechanical strength, high cushioning, good corrosion resistance and low thermal expansion of the fiber reinforced composite materials have allowed its use in the automotive, machine tools, aerospace, sports items[3].

However, the processing of the composites is very difficult to work due to their non-homogenous, anisotropic and reinforced by highly abrasive materials[4]. The composite work piece can cause significant damage and a high wear rate of the cutting tool. After all, the machining of composites depends on various conditions such as the properties of the material[5], the relative content of the reinforcement and the matrix material and the response to the machining process.

Hybrid polymer composites

In polymeric materials, the hybrid is considered to be a type of reinforcing material that is incorporated into a mixture of different matrices, or two or more reinforcing materials and fillers

present in a single matrix or both approaches. When a material has more than two reinforcing stages, the reinforcement of these two phases may lead to positive or negative deviations of the properties predicted by the mix rule and these deviations are known as hybrid effects.

In this thesis, the hybrid polymer composite is made of Graphene Oxide[6]. Graphene Oxide has the characteristics of good thermal stability, which makes it difficult to crack growth and improve the strength and toughness of the composites of the epoxy matrix. Incorporating GO into hybrid composite materials can be considered as the new hybrid epoxy composites that have enormous potential to assist in various applications such as the application of fast machining, aerospace, defense and automotive. A broad classification of composite as matrix and reinforcement[7] is given in **Fig. 1.1**.

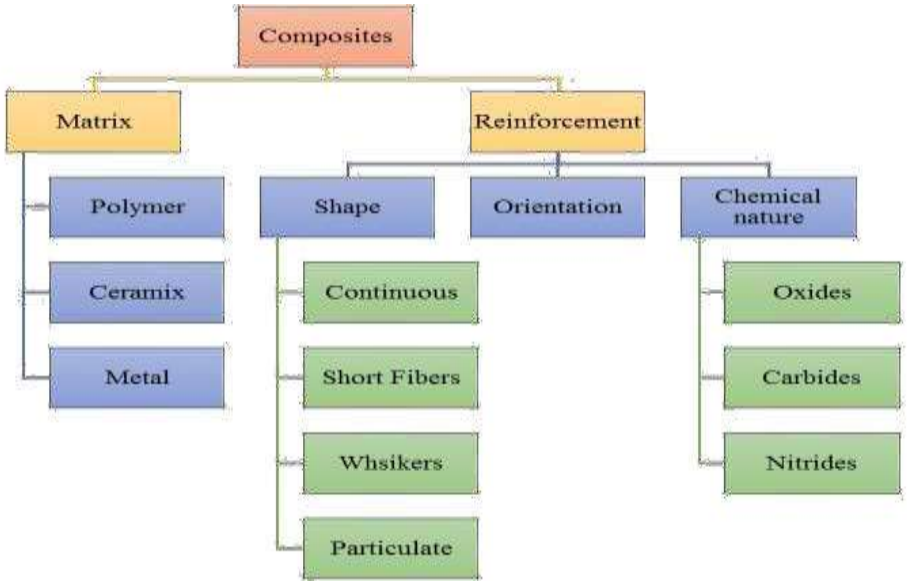

Fig.1.1 Broad classification of composite as matrix and reinforcement

Taguchi method

Experimental design is a powerful analysis tool for modeling and analyzing the influence of output performance control factors[8]. Traditional experimental design is difficult to use, especially when it comes to a large number of experiments and when the number of processing parameters is increasing. The most important aspect in the phase design of the experiment lies in the selection of control factors.

Therefore, the Taguchi method[9], developed by Dr. Genichi Taguchi, is introduced as an experimental technique that allows to reduce the experimental number by using orthogonal matrices and minimizing the effects of control factors. Taguchi is a method that provides a plan of experiments to capture data in a controlled manner by performing these experiments and data analyzes in order to gain information about the behavior of the given process[10]. Further, it is a set of methodologies that the inherent variability of materials and the production process during deer design. It is almost similar to the design of the experiment (DOE), but the balanced experimental (orthogonal) combination of the Taguchi design provides the most efficient fractional factorial design technology. This technique has been applied in the production processes to solve the most confusing problems, especially to observe the degree of influence of the control factors.

In Taguchi's definition, the quality of a product is defined in terms of loss of the product supplied to the company from the moment it is sent to the customer. Losses due to functional variation are known as the losses due to the deviation of the functional characteristics of the product from its desired target value. In addition to this, noise factors are the uncontrollable factors that cause the functional characteristics of a product that does not reach its specific values. The noise factor can be classified as external factors (temperature and human error), manufacturing imperfections and deterioration of the product. The main purpose of quality engineering is to ensure that the

product can be robust with respect to all possible noise factors. Therefore, the Taguchi method could reduce cycle time or product experience, reduce costs by increasing benefits and determining important factors in a shorter period, as it can ensure the quality of the product.

The procedure of the Taguchi design as shown in Fig. 1.2 can be classified into three phases, namely, system design, design parameters and tolerance[11]. The design parameters, considered the most important phase, can determine the factors that influence the quality characteristics in the production process. The first step in the design of the Taguchi parameters is to select the appropriate orthogonal matrix (OA) according to controllable factors. Therefore, the experiments were carried out on the basis of previously established OA and the experimental data were analyzed to identify the optimum condition. Once the optimum conditions identified, the confirmation tests are carried out with the identified optimal levels of all parameters.

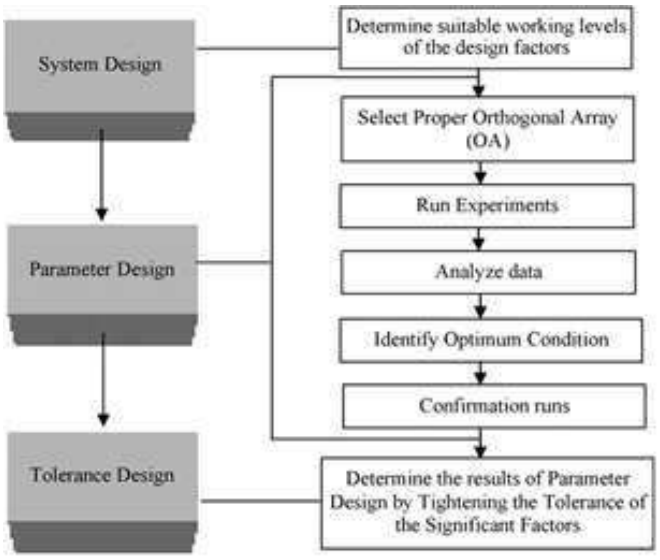

Fig. 1.2 Design procedure of Taguchi

The main objective is quality engineering to produce robust products for all noise factors. So Taguchi created a standard orthogonal array to accommodate as many factors as possible in the control factor selection process to identify non-significant variables on the first occasion. Taguchi has used the signal-to-noise ratio (S / N) as a measurable value of the choice of quality characteristics[12]. This shows that engineering systems can behave in a way that the factors of production can be manipulated into three categories:

- Control factors, (factors that affect the process variability as measured by the S/N ratio).
- Signal factors (factors that do not influence the S/N ratio or process mean).
- Factors (factors that do not affect the S/N ratio or process mean).

1.1 Objective

In this research, Taguchi design parameter phase is the largest design phase and served to determine the finishing fine parameters for obtaining lower surface roughness and cutting force values for the GO- Epoxy composite with different milling parameter conditions. The following are the issues considered in this study:

- The relationship between control factors (cutting depth, spindle speed and feed rate) and output response factors (surface roughness and shear force).
- Optimum conditions for finishing parameters for roughness and cutting strength.

Plan of work

The planning for the project is done as follows:

- Synthesis of Graphene oxide
- FTIR & XRD analysis for the Graphene oxide
- GO-Epoxy Nanocomposite fabrication
- Milling operations on the sample
- Taguchi analysis

1.2 Organization of Thesis

Chapter 1: (Introduction) to provide a brief description of the research background, including the definition of the problem.

Chapter 2: (Literature Review) To provide information of graphene and different testings, graphene oxide history synthesis and its chemical and mechanical properties, various aspects of milling machine.

Chapter 3: (Materials and Methods) to describe the materials and method required for the synthesis of the Graphene oxide along with nano composite of the epoxy-GO, then operations done on the milling machine for optimization by taguchi method

Chapter 4: (Results and Discussion) in this chapter different results of characterization and their speculation have been analysed.

Chapter 5: (Conclusions) provides main outputs of the reseach work

CHAPTER 2

LITERATURE REVIEW

Until 1980s, there were only two well known members of carbon family[13], i.e., graphite and diamond. A great revolution has come with the discovery of other carbon allotropes, viz., fullerenes, CNTs and very recently graphene. Among all these carbonaceous material, graphene has attracted tremendous research interest due to its unique, outstanding properties as well as structural features. Graphene has shown a variety of intriguing properties including superior mechanical properties (intrinsic strength of ~130 GPa), complete impermeability to any gases, ability to sustain extremely high densities of electric current (a million times higher than copper), high electron mobility at room temperature (250,000 cm^2/Vs), exceptional thermal conductivity (5000 $Wm^{-1}K^{-1}$) and easy chemical functionalization comparative to other materials (Table-1)[14]. Moreover, the cost of production of graphene is very low as compared to other carbon-based nanomaterials.

Table 2.1: Properties of graphene, CNT, nano sized steel and polymers

Materials	Tensile strength (GPa)	Thermalconductivity (W/mK)	Electrical conductivity (S/m)
Graphene	160±10	$(4.84\pm0.44)\times10^3$ to $(5.30\pm0.48)\times10^3$	7200
CNT	60-150	3500	3000-4000
Nano sized steel	1769	5-6	1.35×10^6
Plastic (HDPE)	0.018-0.020	0.46-0.52	Insulator
Rubber (Natural)	0.02-0.03	0.13-0.142	Insulator
Fiber (Natural)	3.62	0.04	Insulator

2.1 BACKGROUND OF CARBON MATERIALS

Initially, carbon was discovered by A.L. Lavoisier as charcoal[15] in 1789. It is widely distributed in nature with coal as its main source. Carbon has 4 electrons in four hybridized bonding orbital ($2s^1 2px^1 2py^1 2pz^1$) that are available to form covalent bonds. It is being developed into different allotropes, viz., diamond, graphite, fullerenes, carbon nanotubes and more lately graphene. These allotropes show a variety of interesting electronic and structural properties due to the coexistence of sp^2 and sp^3 hybridized carbon atoms in different proportions.

2.2 GRAPHITE

Graphite is a soft material in which carbon atoms are bonded trigonally with three carbon atoms in the plane as shown in fig 3. Due to such type of bonding, we assume a two dimensional layer type architecture has sp^2 hybridization. Due to intermolecular interactions, these layers stack over each other to form 3D graphitic structure. These layers are bonded by weak Van der Walls forces responsible for the softness of graphite and thus show lubricating properties. The **delocalization of one of the other electrons of each atom forms a π**-cloud due to which graphite is an electrical conductor[16]. The interlayer distance between layers is found to be 3.34Å, with **ABAB…. stacking sequence..**

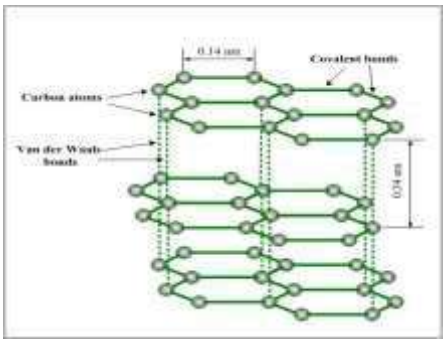

Fig 2.1: General structure of graphite

2.3 DIAMOND

Diamond is an allotrope of carbon with sp^3 hybridized orbitals which are arranged in 3D space to form tetrahedral structure[17] as shown in fig 2.2. Diamond is the hardest known material due to strong covalent bonding. All the orbitals in diamond are filled with no free electron in valence shell due to which diamond is an insulating material with wide band gap. Most of the applications of diamond are related to industrial purpose like grinding, drilling, polishing and cutting due to its unparallel hardness. Besides its suitable refractive index, high optical dispersion and ability to cut along various crystal planes give the diamond its characteristic luster which makes it precious gemstone for jewellery and ornaments.

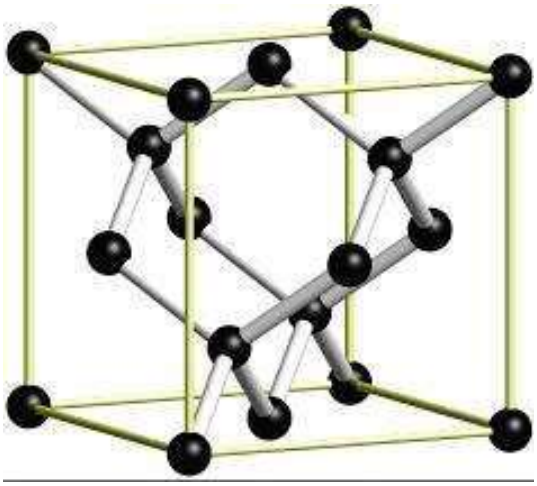

Fig 2.2: General structure of diamond

2.4 FULLERENE

A fullerene is an allotrope of carbon which has many forms such as hollow sphere, tube and many other shapes. Spherical fullerenes, also referred to as Buckminster fullerenes or buckyballs. Fullerenes are similar to graphite is made of stacked graphene sheets of linked hexagonal ring, but they may also have either pentagonal or heptagonal rings[18] as shown in fig 2.3. Buckyballs are subject to intense research, both for their unique chemistry and for their technological applications, especially in nanotechnology, electronics and material science, e.g. , as electron acceptor on photovoltaic, for making inclusion compounds, quantum mechanics studies, super conductivity

Fig 2.3: General structure of fullerene

2.5 CARBON NANOTUBES

Carbon nanotubes[19] (CNTs) are allotropes of carbon which have cylindrical nanostructure as shown in fig 2.4. CNTs are constructed with length-to-diameter ratio of up to 135,000,000:1, considerably larger as compared to any other material. Due to their, surprising mechanical, electrical and thermal properties, carbon nanotubes are used as additives to various structural resources. For example, CNTs are used to manufacture petite portions of the material(s) in some (primarily carbon fiber) golf clubs, bats or automobile parts.. The graphene sheets are rolled at specific and discrete angles, and the combination of the rolling angle and radius decides the nanotube properties; for example, whether the individual nanotube shell is a metal or semiconductor. CNTs are differentiated as single-walled nanotubes (SWNTs) and multi-walled nanotubes (MWNTs). Individual nanotubes naturally align themselves into **"**ropes**"** which are **held together by Van der Waals forces, more specifically, π**-stacking.

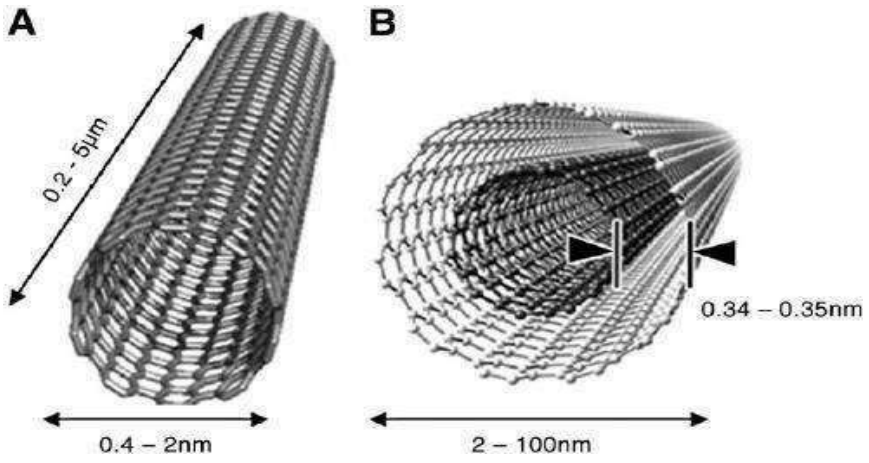

Fig 2.4: Structure of (a) single walled and (b) multi walled CNT

2.6 GRAPHENE

The term graphene first appeared in 1987 to describe single sheets of graphite as one of the constituent of graphite intercalation compounds[19] (GIC). Conceptually, a GIC is a crystalline salt of the intercalant and graphene. The term was also used in early descriptions of carbon nanotubes as well as for epitaxial graphene.

Graphene is a one-atom-thick planar sheet of sp^2 bonded carbon atoms which are densely packed in a honeycomb shaped lattice. In a 2-D carbon system for graphene, three carbon electrons from four hybridized bonding electrons form strong in-plane sp^2 bonds consisting of the honeycomb structure, and a fourth electron spreads out over the top or bottom of the layer as a π electron[20].

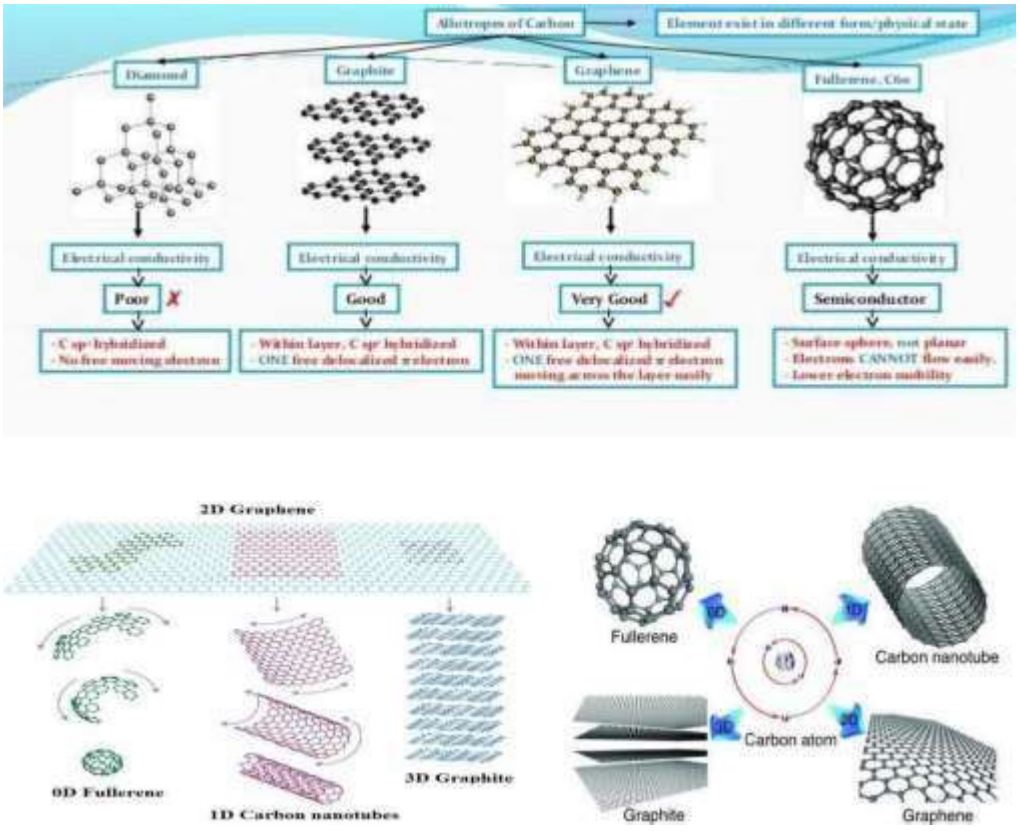

Fig 2.5: Graphene and its relation to fullerene, CNT and graphite

2.7 Fourier Transformation Infra Red Spectroscopy (FTIR)

FT-IR stands for Fourier Transform Infra Red, the preferred method of infrared spectroscopy. In infrared spectroscopy, IR radiation is passed through a sample[21]. Some of the infrared radiation is absorbed by the sample and some of it is passed through (transmitted). The resulting spectrum represents the molecular absorption and transmission, creating a molecular fingerprint of the sample. Like a fingerprint no two unique molecular structures produce the same infrared spectrum[22]. This makes infrared spectroscopy useful for several types of analysis. So, what information can FT-IR provide?

•It can identify unknown materials

•It can determine the quality or consistency of a sample

•It can determine the amount of components in a mixture

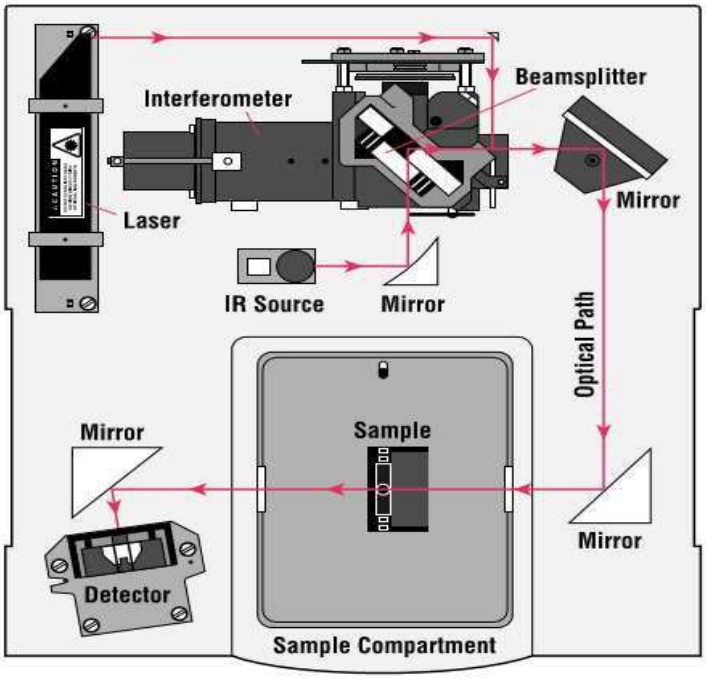

Fig. 2.6 Layout of a spectrophotometer

Analysis process of FTIR

The normal instrumental process is as follows:

1. **The Source**: Infrared energy is emitted from a glowing black-body source. This beam passes through an aperture which controls the amount of energy presented to the sample (and, ultimately, to the detector).

2. **The Interferometer**: The beam enters the interferometer where the ―spectral encoding‖ takes place. The resulting interferogram signal then exits the interferometer.

3. **The Sample**: The beam enters the sample compartment where it is transmitted through or reflected off of the surface of the sample, depending on the type of analysis being accomplished. This is where specific frequencies of energy, which are uniquely characteristic of the sample, are absorbed.

4. **The Detector**: The beam finally passes to the detector for final measurement. The detectors used are specially designed to measure the special interferogram signal.

5. **The Computer**: The measured signal is digitized and sent to the computer where the Fourier transformation takes place. The final infrared spectrum is then presented to the user for interpretation and any further manipulation and can be seen in the fig.2.7.

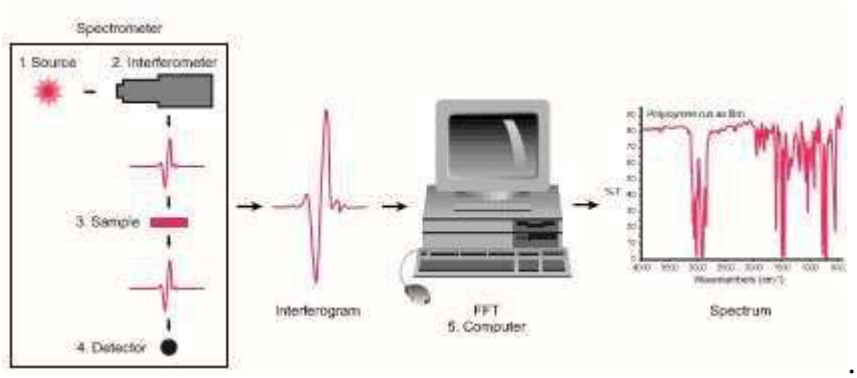

Fig.2.7 sample process for FTIR

2.8 Scanning Electron Microscopy (SEM)

A scanning electron microscope[2] (SEM) is a type of electron microscope that produces images of a sample by scanning the surface with a focused beam of electrons. The electrons interact with atoms in the sample, producing various signals that contain information about the sample's surface topography and composition. The electron beam is scanned in a raster scan pattern, and the beam's position is combined with the detected signal to produce an image. SEM can achieve resolution better than 1 nanometer. Specimens can be observed in high vacuum in conventional SEM, or in low vacuum or wet conditions in variable pressure or environmental SEM, and at a wide range of cryogenic or elevated temperatures with specialized instruments.

The most common SEM mode is detection of secondary electrons emitted by atoms excited by the electron beam. The number of secondary electrons that can be detected depends, among other things, on specimen topography. By scanning the sample and collecting the secondary electrons that are emitted using a special detector, an image displaying the topography of the surface is created.

Scanning process and image formation

In a typical SEM, an electron beam is thermionically emitted from an electron gun fitted with a tungsten filament cathode[24]. Tungsten is normally used in thermionic electron guns because it has the highest melting point and lowest vapor pressure of all metals, thereby allowing it to be electrically heated for electron emission, and because of its low cost. Other types of electron emitters include lanthanum hexaboride (LaB6) cathodes, which can be used in a standard tungsten filament SEM if the vacuum system is upgraded or field emission guns (FEG), which may be of the cold-cathode type using tungsten single crystal emitters or the thermally assisted Schottky type, that use emitters of zirconium oxide[25].

The electron beam, which typically has an energy ranging from 0.2 keV to 40 keV, is focused by one or two condenser lenses to a spot about 0.4 nm to 5 nm in diameter. The beam passes through pairs of scanning coils or pairs of deflector plates in the electron column, typically in the final lens, which deflect the beam in the x and y axes. The SEM that is used in general laboratories can be seen in figure 2.8.

Fig.2.8 Pictorial view of SEM machine

2.9 X-Ray Diffraction (XRD)

X-ray Diffraction is a technique used for determining the atomic and molecular structure of a crystal, in which the crystalline atoms cause a beam of incident X-rays to diffract into many specific directions. By measuring the angles and intensities of these diffracted beams, a crystallographer can produce a three-dimensional picture of the density of electrons within the crystal. From this electron density, the mean positions of the atoms in the crystal can be determined, as well as their chemical bonds, their disorder, and various other information.

Since many materials can form crystals—such as salts, metals, minerals, semiconductors, as well as various inorganic, organic, and biological molecules—X-ray crystallography has been fundamental in the development of many scientific fields. In its first decades of use, this method determined the size of atoms, the lengths and types of chemical bonds, and the atomic-scale differences among various materials, especially minerals and alloys. The method also revealed the structure and function of many biological molecules, including vitamins, drugs, proteins and nucleic acids such as DNA. X-ray crystallography is still the chief method for characterizing the atomic structure of new materials and in discerning materials that appear similar by other experiments. X-ray crystal structures can also account for unusual electronic or elastic properties of a material, shed light on chemical interactions and processes, or serve as the basis for designing pharmaceuticals against diseases.

X-ray crystallography shows the arrangement of water molecules in ice, revealing the hydrogen bonds in Fig.2.9 that hold the solid together[26]. Few other methods can determine the structure of matter with such precision.

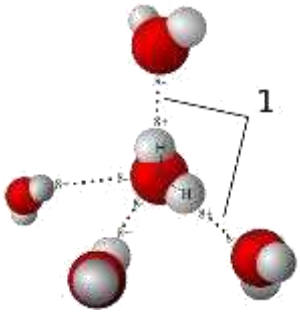

Fig. 2.9 Arrangement of water molecules in ice

X-ray crystallography is related to several other methods for determining atomic structures. Similar diffraction patterns can be produced by scattering electrons or neutrons, which are likewise interpreted by Fourier transformation. If single crystals of sufficient size cannot be obtained, various other X-ray methods can be applied to obtain less detailed information; such methods include fiber diffraction, powder diffraction and (if the sample is not crystallized) small-angle X-ray scattering (SAXS). If the material under investigation is only available in the form of nanocrystalline powders or suffers from poor crystallinity, the methods of electron crystallography can be applied for determining the atomic structure.

2.10 Milling Machine

Fig 2.10. Pictorial view of the milling machine

Milling is the machining process of using rotary cutters to remove material from a workpiece by advancing (or feeding) in a direction at an angle with the axis of the tool. It covers a wide variety of different operations and machines, on scales from small individual parts to large, heavy-duty gang milling operations. It is one of the most commonly used processes in industry and machine shops today for machining parts to precise sizes and shapes.

Milling can be done with a wide range of machine tools[27]. The original class of machine tools for milling was the milling machine (often called a mill). After the advent of computer numerical control (CNC), milling machines evolved into machining centers (milling machines with automatic tool changers, tool magazines or carousels, CNC control, coolant systems, and enclosures), generally classified as vertical machining centers (VMCs) and horizontal machining centers (HMCs). The integration of milling into turning environments and of turning into milling environments, begun with live tooling for lathes and the occasional use of mills for turning operations[28], led to a new class of machine tools, multitasking machines (MTMs), which are purpose-built to provide for a default machining strategy of using any combination of milling.

2.11 TAGUCHI ANALYSIS

Different machining processes were optimized by the researchers to improve the quality of the tool G.Akhyar et al[29]. applied Taguchi optimization method for the optimization of cutting parameters in turning Ti-6%, Al-4% with coated and uncoated cemented carbide tools under dry conditions and high cutting speeds for better surface roughness. L27 orthogonal array including four factors such as Cutting speed, feed rate, depth of cut and tool grades with three levels for each factor was used to identify the optimal combination. They used ANOVA to determine the cutting speed and tool grade to be a significant factor that affected the surface finish M.Y. Noordin et al. used RSM to study the performance of a multilayer tungsten carbide tools while turning AISI 1045 steel with constant depth of cut and feed rate. To study the effects of three factors such as cutting speed, feed and side cutting edge angle (SCEA) on surface roughness and the tangential force using face centered CCD. There are other factors that provide secondary contributions to the performance indicators. In the case of surface roughness, the SCEA2 and the interaction of feed and SCEA provides these contributions whilst for tangential force, the SCEA2,the interaction of feed and SCEA; and the cutting speed provides them. Hari Vasudevan et al. used Taguchi method to optimize the milling parameters on Glass Fibre Reinforced Plastic NEMA 11[30]. In this study, an attempt has been made to optimize milling parameters with multiple performance characteristics, based on the Grey Relational Analysis coupled with Taguchi method. The milling experiments were carried out on a vertical Milling machine.

The experiments were conducted according to L18 (OA). The four cutting parameters selected for this investigation are milling strategy, spindle speed, feed rate and depth of cut. Mohammed T. Hayajneh et al. build a multiple regression model for surface roughness to study the effects of

spindle speed, cutting feed rate, depth of cut and their two way interactions. The cutting parameters were selected as four levels of cutting speed, seven levels of feed rate and three levels of depth of cut. The results showed the cutting feed as the most dominant factor and interactions cutting feed-depth of cut, and cutting feed-spindle speed the most significant. Ghhani J. A. *et al*. optimized cutting parameters in end milling process while machining hardened steel AISI H13 with TiN coated P10 carbide insert tool under semi-finishing and finishing conditions of high speed cutting[31]. The effect of milling parameters such as cutting speed, feed rate and depth of cut along with their interactions on the process is studied using Taguchi method of experimental design (DOE).The study indicated the suitability of Taguchi method to solve the stated problem with minimum number of trials as compared with a full factorial design. Shreemoy Kumarnayak *et al*. The Investigation was carried out the effect of machining parameters during dry turning of AISI 304 austenitic stainless steel[32]. For this study HMT heavy duty lathe machine was used. They have adopted L27 orthogonal array with three machining parameters like cutting speed, feed rate and depth of cut and three importance characteristics of machinability such as material removal rate (MRR), cutting force and surface roughness (R_a) were measured.

CHAPTER 3

MATERIALS AND METHODS

3.1 RAW MATERIALS

- Graphite powder (CHD, India)
- Sodium nitrate $NaNO_3$ (Fischer scientific)
- Potassium permanganate $KMnO_4$ (Fischer scientific)
- Sulphuric acid H_2SO_4, 98% (Merck chemicals)
- Hydrogen peroxide H_2O_2, 30% (Speck pure chemicals)
- Epoxy
- TETA (as a hardener)

3.2 SYNTHESIS OF GO

- To prepare GO using Hummer's Method[33], we took a clean dry beaker and rinsed it using concentrated sulphuric acid.
- Take 75ml of H_2SO_4 and then added 3gm of $NaNO_3$. Stirred this solution for 1 h, then added 3gm of graphite and stirred for 3 h.
- We added 9gm of $KMnO_4$ very slowly while keeping it on an ice bath so that the temperature of the solution does not rise above 20 C.
- Stirred this solution on a magnetic stirrer for 24 h.

- Then added 150 ml of water to this solution and stirred for 20 min and then added 420ml of water and stirred for 10 min.
- Then we added H_2O_2 to the solution till a bright yellow color is obtained.
- Then filtered the solution and washed the precipitate with water 2-3 times or till all the acid is removed. Centrifuged the solution and the GO pulp is removed.
- We put the GO pulp in oven for 5-6 h and collect the powder in eppendorf.

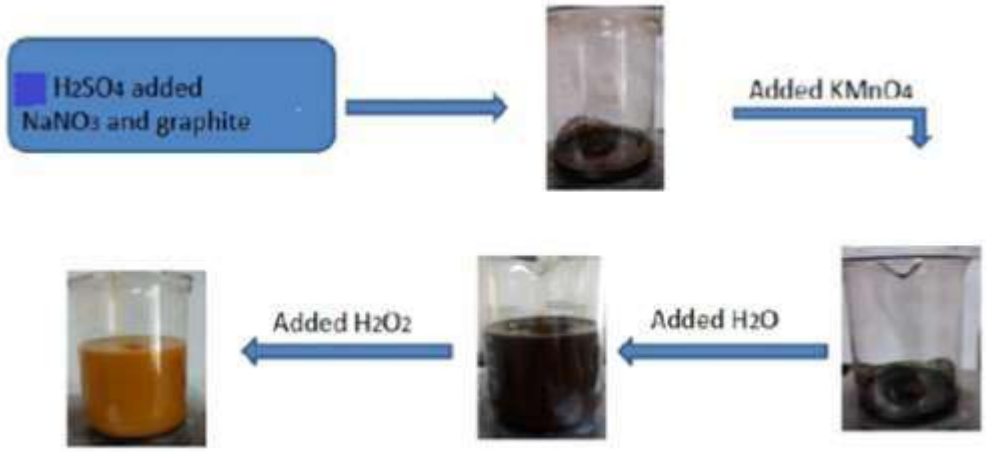

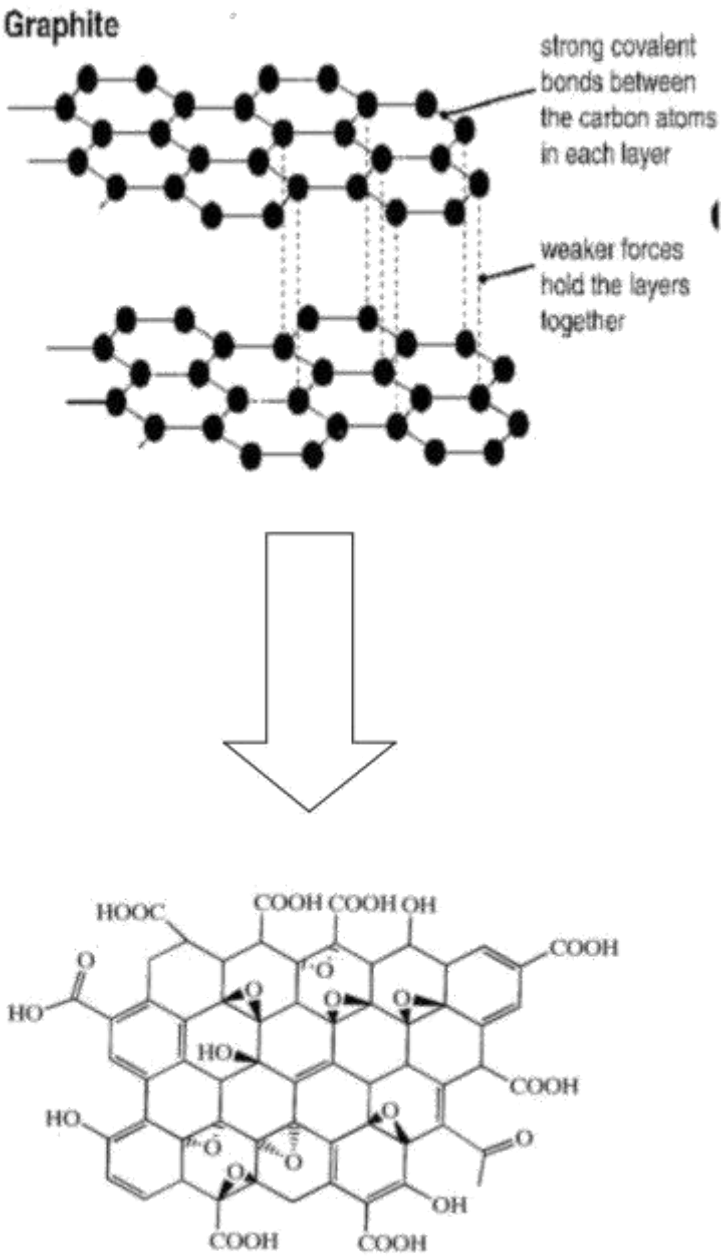

Fig 3.1: Oxidisation of Graphite

(a)

(b)

(c)

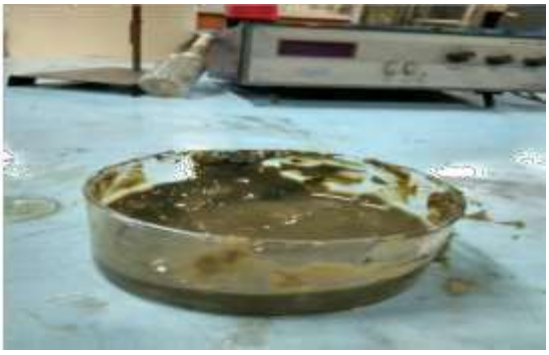

(d)

(e)

(f)

Fig 3.2 : Different phases of synthesis GO (a)&(b) solution on the magnetic stirrer after adding graphite (c) solution on ice bath (d) pulp after centrifuge (e) nanocomposite pulp after 5 h (f) GO in eppendrof in powdered form.

3.3 SAMPLE PREPARATION

- Clean the mold and dry it completely.
- Weigh 100 g of epoxy resin and pour it in a beaker.
- Weigh 1 g of hardner and pour it in a different beaker.
- Weigh graphene oxide according to desired concentrations (1% of 110 g)
- Mix graphene oxide with epoxy resin followed by hardener.
- Finally with the help of brush pour the mixture of resin, hardner and GO over the mold.
- Make sure that mold surface is coated with release agents like Vaseline for easy removal of sample.
- Keep the sample for 24 h for curing.
- After curing is done, safely take the sample out.
- Sample dimension: 114x88x8 mm^3

(a)

(b)

(c)

(d)

Fig 3.3. Different stages of sample preparation (a,b,c,d)

3.4 MILLING OPERATION

- The sample was machined in the project shop of the mechanical engineering department.
- The sample was first made ready to clamp on the milling machine.
- File and clamp were used to make the sample suitable for the milling as shown in fig. 16.
- The rectangular sample made up of GO-Epoxy composite was fitted to milling machine.
- Slots of width 5mm was only available for the working.

Fig 3.4. Preparing sample for the milling machine

- For taguchi optimization , we need three different factors for the optimization.
- In this research, we are taking feed rate(f), spindle speed (s), and depth of cut(d) as three factors on which optimization need to be done.
- Feed rates were taken as 20, 40,60 (mm/min)
- Depth of cut were taken as 0.4, 0.6, 0.8 (mm)
- Spindle speed were 500, 1000, 1500 (rpm)
- 27 slots were made on the sample of length 20 mm each.

Fig 3.5. Machining on the neat sample

Fig 3.6. Machining on the GO-epoxy Sample

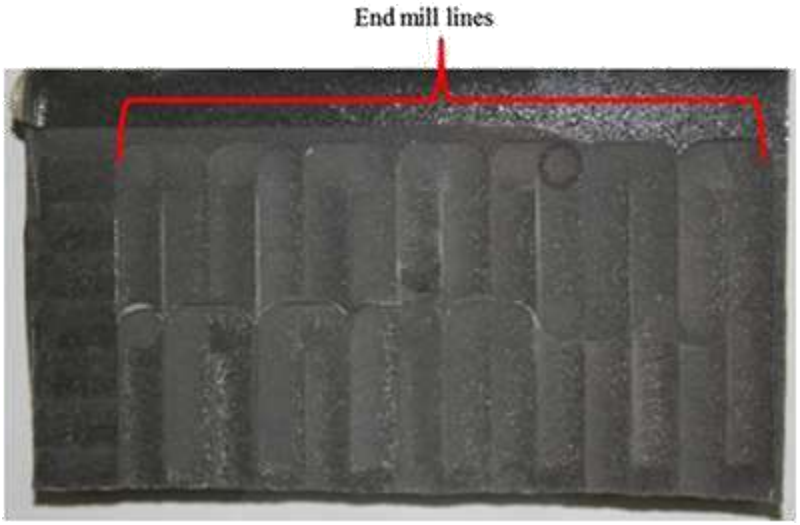

Fig 3.7. Slots cutting on the sample

In this experiment twenty seven different combinations of milled lines with 6 mm width were made by performing an end-milling operation (dry condition) on the hybrid composite sample as shown in fig 3.7. The milling operation processes were performed in milling centre. Meanwhile, the cutting tool used is the NKO end-milling tool with four flutes (dia, 6 mm). The surface roughness measurement was done by using a portable surface roughness tester TR200 (measures R_a in lm; stylus travel 1.5 mm cut-off). Be-sides that, the cutting forces were also measured online during end-milling operation with a sensitive three component Kistler 5070A type piezoelectric dynamometer with a charge amplifier. The data acquisition was made through the charge amplifier and a computer using the appropriate software (Dynoware). The microsurface morphology study was carried out using the Scanning Electron Microscope Hitachi S-3400N.

CHAPTER 4

RESULTS AND DISCUSSION

4.1 Fourier Transform Infra Red Spectroscopy

The FTIR spectra have been used to measure, how well the sample absorbs the light at which wavelength, by using this we can find out, which functional group is present in the material.

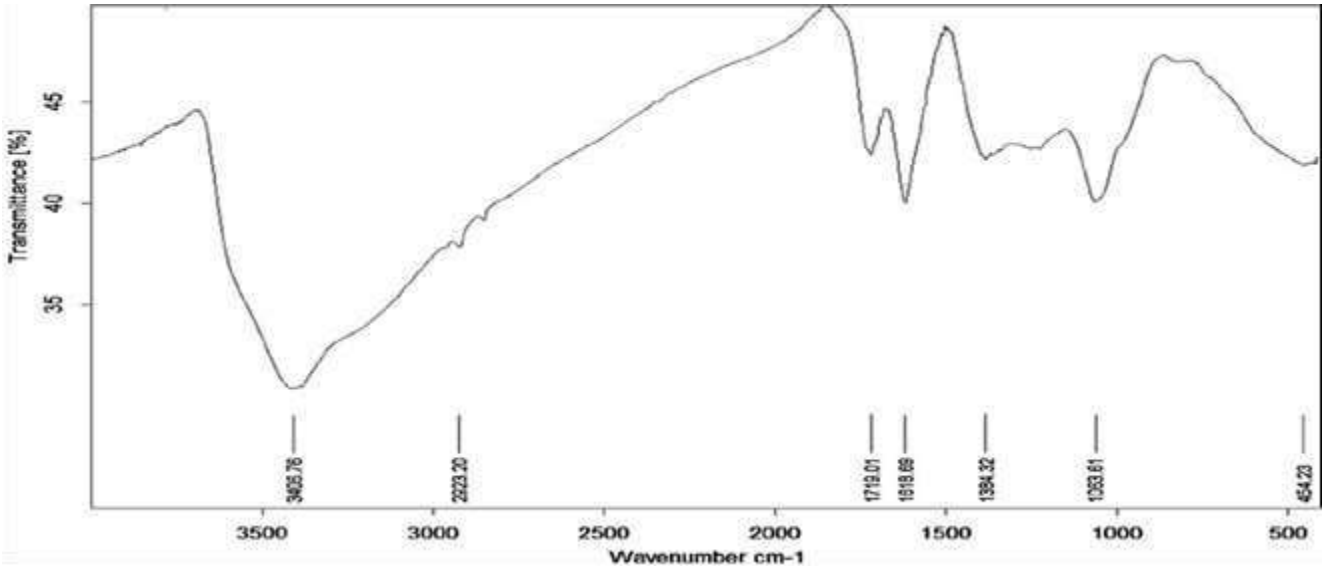

Fig 4.1. : FTIR spectra of graphite oxide

GO nanocomposite. A prominent peak adsorption appeared at 3407 cm^{-1} reveals the vibration of the hydroxyl group (O-H) present in GO. This OH-bond may be due to the presence of alcohol, phenol, carboxylic acids and so on.

Due to the presence of water at this vibration frequency also confirms the prepared hydrophilic properties of GO. In addition, the upper parts (1696, 1233 and 1064) cm^{-1} of the carbonyl group (C = O), the Epoxy and alkoxy groups. The C = C is present in the 1.627 cm^{-1} band that gives the signature of the carbon groups do not oxidize.

4.2 Powder X-Ray Diffraction Analysis

X-ray diffraction is an analytical tool used to identify the atomic and molecular structure of the crystals in which the incident beam is diffused in many directions. Looking at the intensities and angles of the diffracted beam can give a 3-D image of the electronic density in the crystal and thus use this information, we can determine the various chemical bonds, a crystal disorder, and much more information about the crystal plane. In our current study, we performed the synthesized GO and compared the untreated graphite. The XRD spectra are measured in the range of 2Ɵ i.e to 5 , showing a peak of graphite diffraction at a 26 angle is the distance between the layers is then calculated using the Brags equation, that is, Sin2d = Nλ.

That s almost equal to 3.34 for graphite. While the oxygen functionality group introduced in graphite, there is an expansion of the graphite layers and the separation between graphite increases, so the diffraction angle must be lower. It is clearly observed in the XRD spectra of GO that the angle of diffraction of GO is at a 12° angle and, therefore, the separation between the peaks is almost equal to 7.97

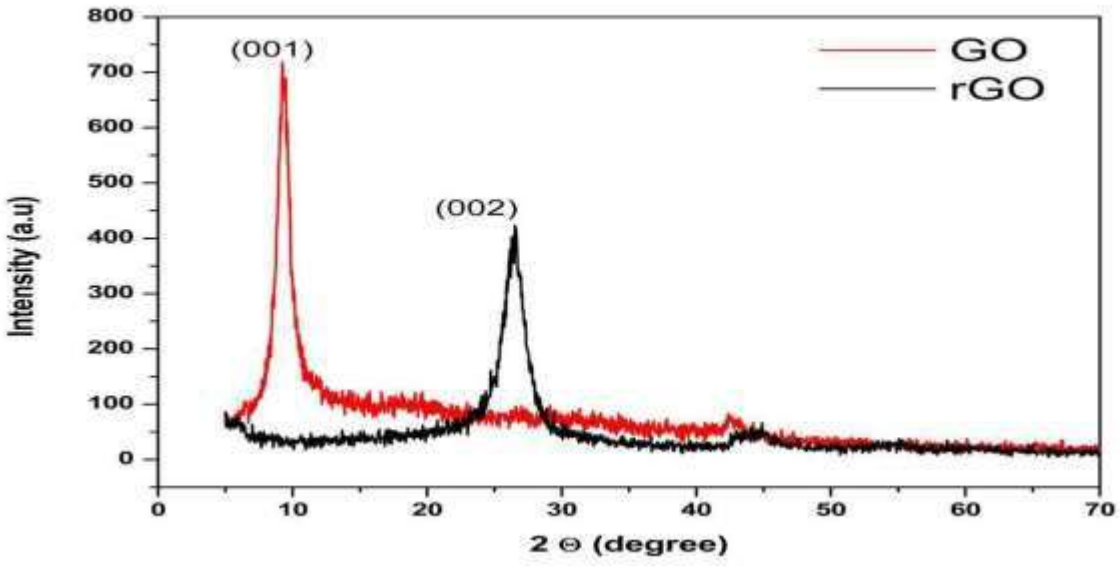

Fig 4.2: XRD pattern of graphine oxide (GO) and reduced graphene oxide (rGO)

4.3 TAGUCHI ANALYSIS: Orthogonal array and experimental factors

In the design phase of the Taguchi method parameters in the figure 2, the first step is to configure and select an appropriate orthogonal array[34].

Table 4.1.The basic Taguchi $L_{27}(3^3)$ orthogonal array.

Run	Control factors and levels		
	A	B	C
1	1	1	1
2	1	1	2
3	1	1	3
4	1	2	1
5	1	2	2
6	1	2	3
7	1	3	1
8	1	3	2
9	1	3	3
10	2	1	1
11	2	1	2
12	2	1	3
13	2	2	1
14	2	2	2
15	2	2	3
16	2	3	1
17	2	3	2
18	2	3	3
19	3	1	1
20	3	1	2
21	3	1	3
22	3	2	1
23	3	2	2
24	3	2	3
25	3	3	1
26	3	3	2
27	3	3	3

Table 4.2 Parameters, codes, and level values used for orthogonal array

Parameter	Code	Level 1	Level 2	Level 3
Control factors				
Depth of cut, d (mm)	A	0.4	0.6	0.8
Spindle speed, S (rpm)	B	500	1000	1500
Feed rate, f (mm/pm)	C	20	40	60
Response variable				
Surface roughness, Ra (lm)	–	–	–	–
Cutting force, Fr (N)	–	–	–	–

To accommodate three control factors into the experimental study, a standardized Taguchi-based experiment design, L27 was chosen to be used in this study and is shown in Table 4.1. This basic design makes use of three control factors with three levels each and the design has capability to check the interaction between the factors. From the standard design (Table 4.1), there are 27 experimental runs that need to be conducted with the combination of levels for each control factor (A–C). As the incorporation of the noise factors into the OA is optional, the noise factor is omitted from this experimental study. The selected parameters are displayed in Table 4.1 together with their codes and values for the application in Taguchi parameter design study. In this study, the control factors (Depth of cut, Spindle speed, and Feed rate) are the independent variables while the response factors (Surface roughness, Cutting force) are the dependent variables. In Table 4.3, a modified OA has been created by using basic Taguchi OA (Table4.2) and the selected parameters from Table 4.1. In this modified OA, the basic arrays of control factors are combined with the arrays of response factors along with the S/N ratio (g) values and it brings to the total number of 27 experimental runs.

Table 4.3. Orthogonal array

Run	Inner control factor array			R_a	g_{Ra}	F_r	g_{Fr}
	A	B	C				
1	1	1	1	1.15	1.21	94.31	39.49
2	1	1	2	1.94	5.74	41.54	32.37
3	1	1	3	1.18	1.47	38.87	31.79
4	1	2	1	0.96	0.34	16.44	24.32
5	1	2	2	0.62	4.15	5.45	14.73
6	1	2	3	0.77	2.25	35.85	31.09
7	1	3	1	1.06	0.48	43.78	32.83
8	1	3	2	0.36	8.95	35.46	30.99
9	1	3	3	0.29	10.84	83.02	38.38
10	2	1	1	1.43	3.12	60.28	35.60
11	2	1	2	0.89	1.01	1.63	4.23
12	2	1	3	1.28	2.14	45.85	-33.23
13	2	2	1	1.10	0.82	12.76	22.12
14	2	2	2	0.86	1.36	7.57	17.58
15	2	2	3	0.77	2.23	23.60	27.46
16	2	3	1	0.37	8.71	9.46	19.52
17	2	3	2	0.63	3.97	4.81	13.64
18	2	3	3	0.84	1.55	47.63	33.56
19	3	1	1	1.14	1.12	3.13	9.92
20	3	1	2	1.80	5.08	62.40	35.90
21	3	1	3	1.81	5.16	93.45	39.41
22	3	2	1	1.15	1.22	41.94	32.45
23	3	2	2	1.43	3.08	2.27	7.11
24	3	2	3	2.11	6.47	42.31	32.53
25	3	3	1	0.95	0.47	8.41	18.50
26	3	3	2	1.25	1.94	23.51	27.42
27	3	3	3	0.47	6.54	14.23	23.06
	A	B	C				
R_a Effects							
Level 1	0.93	1.40	2.92				
Level 2	0.91	1.08	1.08				
Level 3	1.34	0.69	1.06				
g_{Ra} Effects							
Level 1	1.96	2.67	0.17				
Level 2	1.42	0.14	0.40				
Level 3	1.89	4.29	0.91				
F_r Effects							
Level 1	43.86	49.05	32.28				
Level 2	23.73	20.91	20.52				
Level 3	32.41	30.03	47.20				
g_{Fr} Effects							
Level 1	30.67	29.10	-26.08				
Level 2	22.99	23.27	20.44				
Level 3	25.14	26.43	32.28				

Data analyzing on the optimal levels for all control factors is the first step after completing the experimental stage. The main aim for this experiment is to optimize the milling parameters to obtain lower surface roughness and optimum resultant cutting force values so the smaller the better characteristic was chosen in this analysis. The results from the experimental stage which are the surface roughness, R_a and cutting force, Fr values are recorded in Table 4. Conceptual S/N approach is recommended by Taguchi for the means and S/N ratio analysis which involves graphing the effects and visually identifying the factors which appear to be significant without using ANOVA analysis. Thus, these made the approach to become more simple and effective.

Determination of the optimum machining parameters.

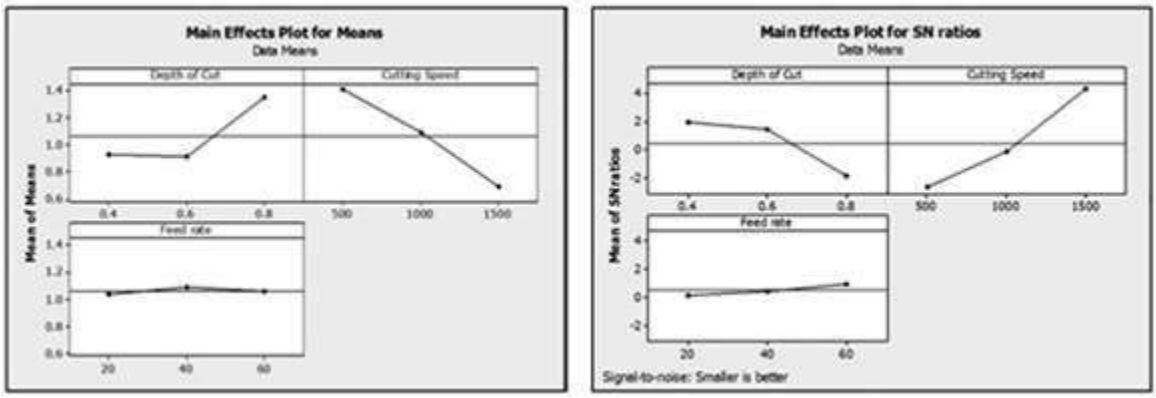

Fig. 4.3 Ra means and S/N ratio effects for each control factors

- **Surface roughness**

The-smaller-the-better characteristic was used to determine the smallest surface roughness (R_a) that would be the ideal situation for this study. Meanwhile, the larger S/N ratio would be projected as the best response given in the machine set-up system which would be the ideal situation. The graphs in Fig. 22 are used to determine the optimal set of parameters from this experimental design. From the graphs, the control factor of depth of cut (A) at level 1 (0.4 mm) shows the best result. On the other hand, the cutting speed control factor (B) provides the best

result at the level 3 (1500 rpm). Meanwhile, the feed rate control factor (C) gives the best results at the level 3 (60 mm/min). There are no conflicts in determining the optimal depth of cut, spindle speed and feed rate and the criteria of the lowest response and highest S/N ratio were followed. Thus, the optimized combination of levels for all the three control factors from the analysis which provides the best surface finish was found to be A1–B3–C3.

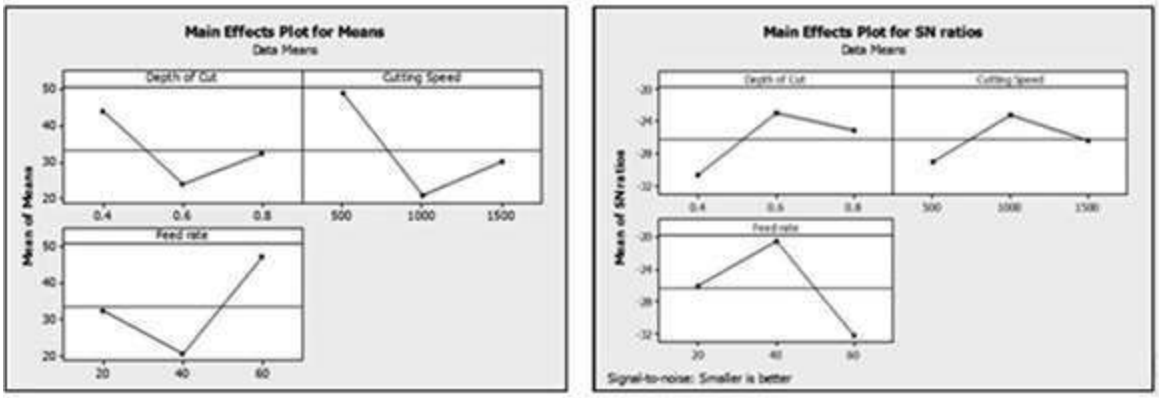

Fig. 4.4 Fr means and S/N ratio effects for each control factors.

- **Cutting force**

In the other response factors, the resultant cutting force (Fr), the-smaller-the-better characteristic was used and the smallest resultant cutting force value would be the ideal situation. The control factor of depth of cut (A) at level 2 (0.6 mm) showed the best result. Besides that, the cutting speed control factor (B) provided the best result at the level 2 (1000 rpm). On the other hand, the feed rate control factor (C) showed the best results at the level 2 (40 mm/pm). There were also no conflicts happening in determining the optimal depth of cut, spindle speed and feed rate while the criteria of the lowest response and highest S/N ratio were followed.

Thus, the optimized combination of levels for all the three control factors from the analysis which provides the lowest cutting force was found to be A2–B2–C2.

4.5 MORPHOLOGY STUDY

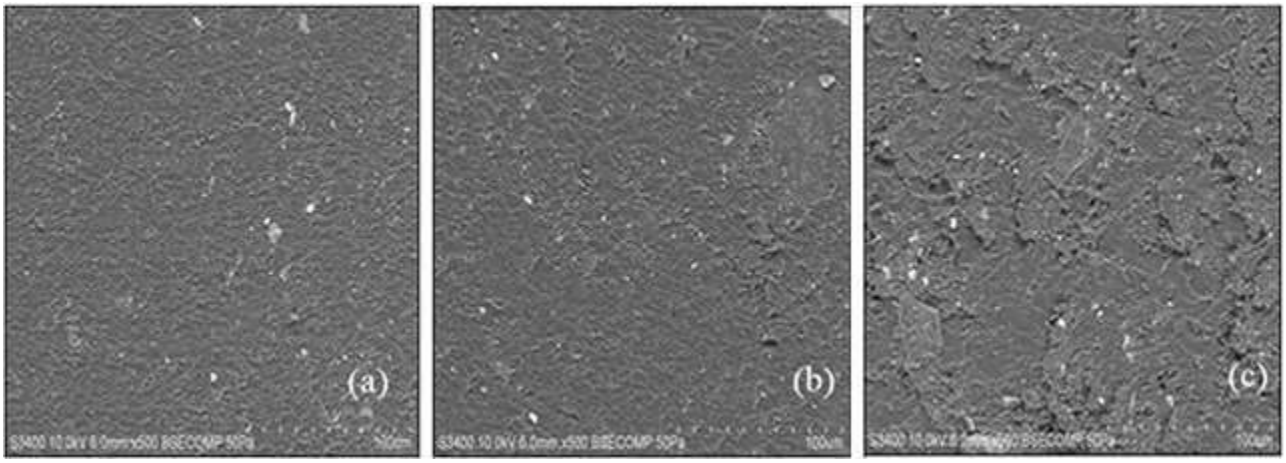

Fig 4.5. SEM Surface morphology study. (a) Lowest R_a (b) medium R_a and (c) highest Ra.

From the analysis of surface roughness, there are three optimal combinations of control factors which give three different responses in surface roughness value that can be identified. The first control factor combination which gives lowest surface roughness value is A1–B3–C3. Meanwhile, the second control factor combination of A2–B2–C2 gave a medium surface roughness value (R_a). For the third combination of the control factors, A3–B1–C1 gives the highest surface roughness value (R_a).In Fig. 4.5, the surface morphology studies were done on all three optimum surfaces. From the study, the surface morphology images in terms of roughness for all three machining lines can be seen to be varied following the variation of surface roughness value.

4.6 Material Removal Rate (MRR)

The material removal rate was obtained by a 3x3 array by keeping spindle speed constant. The levels are shown in table 4.4.

Table 4.4. Parameters for orthogonal array

LEVEL	DEPTH OF CUT	FEED RATE
1	0.4	20
2	0.6	40
3	0.8	60

The result obtained for MRR can be seen in table 4.5 by the multiplication of depth of cut and feed rate.

Table 4.5. Orthogonal array

Exp.No	DEPTH OF THE CUT	FEED RATE	MRR
1	0.4	20	48
2	0.4	40	96
3	0.4	60	144
4	0.6	20	72
5	0.6	40	144
6	0.6	60	216
7	0.8	20	96
8	0.8	40	192
9	0.8	60	288

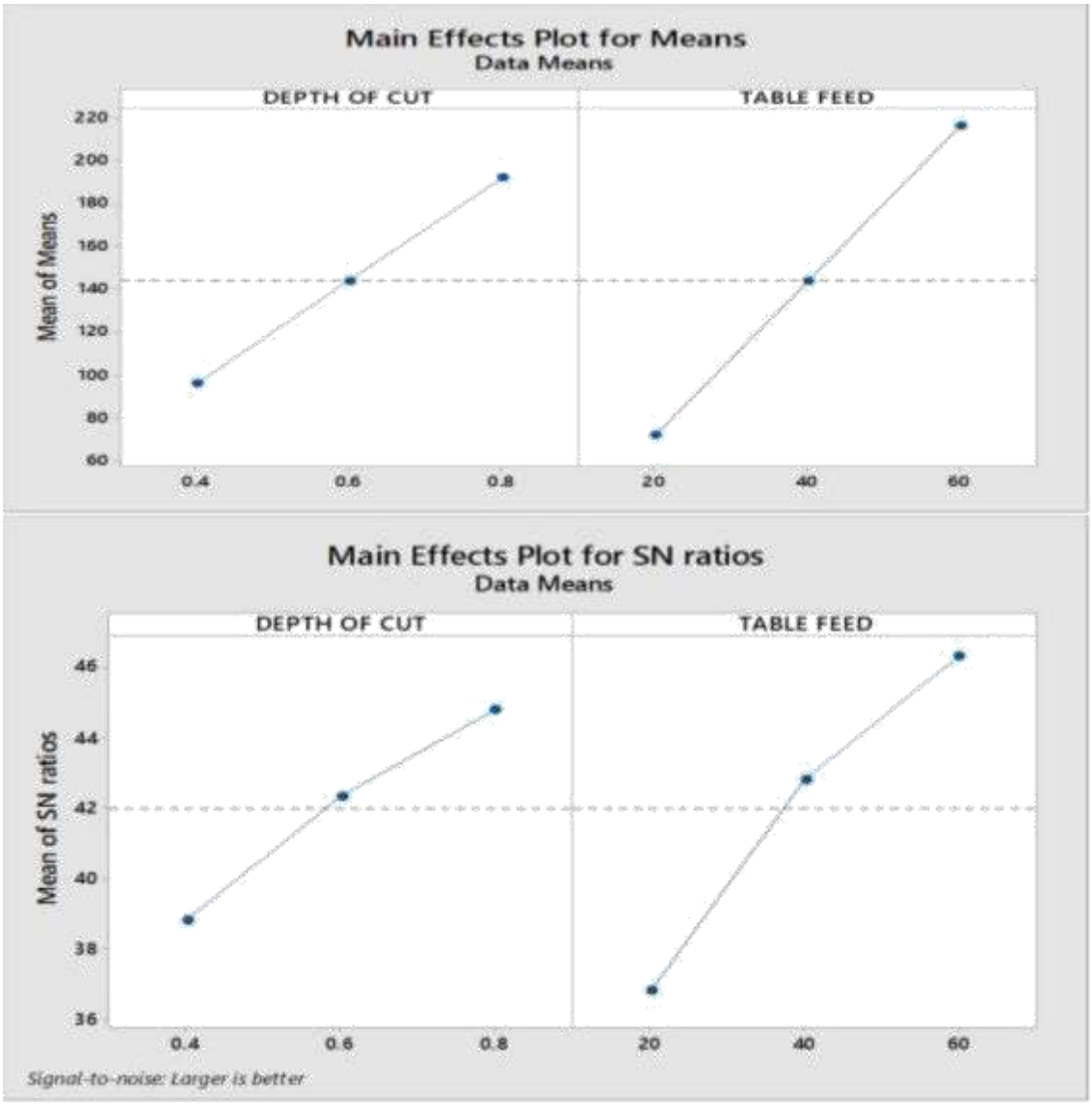

Fig. 4.6 MRR means and S/N ratio effect for various factor

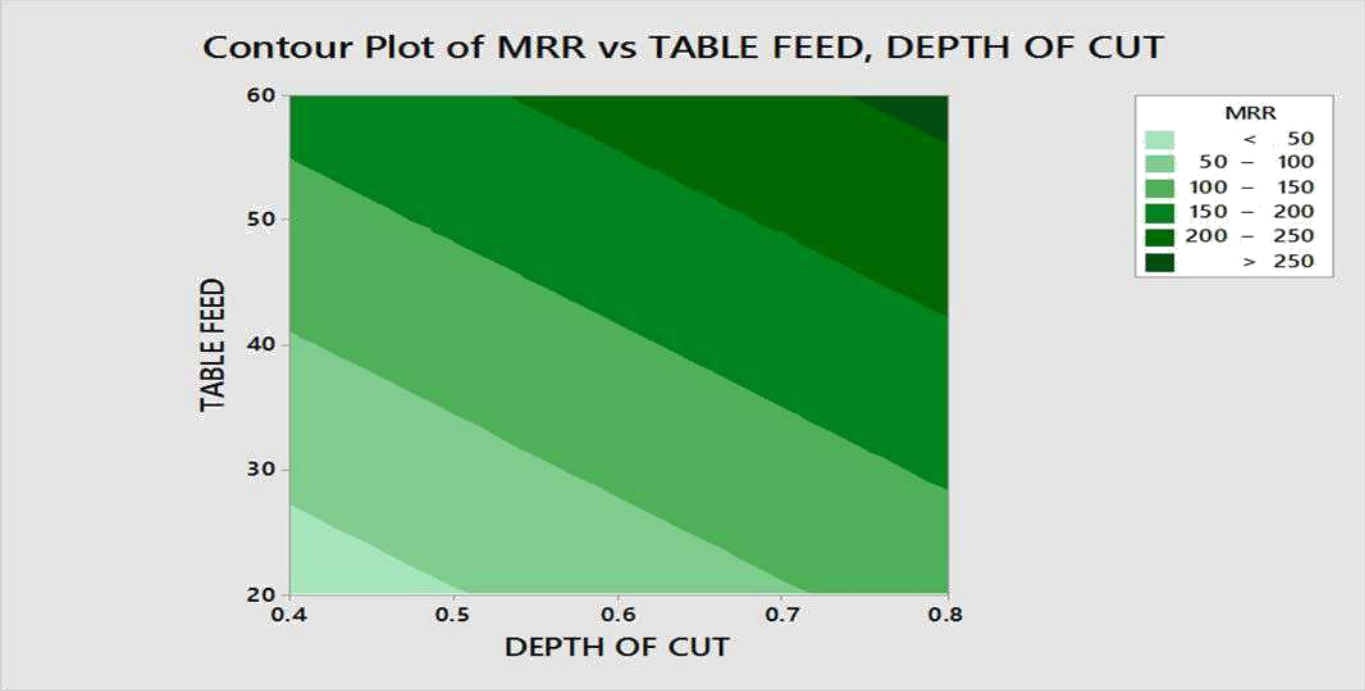

Fig.4.7 Contour plot of MRR vs Table feed, depth of cut

Analysis of Variance (ANOVA)

Source	DF	Adj SS	Adj MS	F-Value	P-Value
Regression	2	44928	22464.0	58.50	0.000
DEPTH OF CUT	1	13824	13824.0	36.00	0.001
TABLE FEED	1	31104	31104.0	81.00	0.000
Error	6	2304	384.0		
Total	8	47232			

PERCENTAGE CONTRIBUTION OF INDIVIDUAL FACTORS

Depth of cut---- 30.769 %

Table feed -----69.230 %

REGRESSION EQUATION USING ANOVA: -

MRR = -144.0 + 240.0 DEPTH OF CUT + 3.600 TABLE FEED

CHAPTER 5

CONCLUSIONS

Graphene oxide nanocomposite have been successfully synthesized at optimized conditions. FTIR and XRD clearly reveals the successful formation of GO. Machining i.e milling was done easily on the nanocomposite and taguchi analysis was performed to check the optimal cutting parameters from different levels and combinations. After receiving all the result we can now conclude that taguchi analysis is an efficient way to determine the optimal combination for lowest surface finish, material removal rate and cutting force. Additionally, the micro-structure surface morphology study was presented on the visual variation of machined surface roughness which seems to be identical to the variation of surface roughness value.

REFERENCES

1. Liu, Sen, Jingqi Tian, Lei Wang, Hailong Li, Yingwei Zhang, and Xuping Sun. "*Stable aqueous dispersion of graphene nanosheets: noncovalent functionalization by a polymeric reducing agent and their subsequent decoration with Ag nanoparticles for enzymeless hydrogen peroxide detection*." Macromolecules 43, no. 23 **(2010):** 10078-10083.
2. Dimitrakakis, G. K., Tylianakis, E., & Froudakis, G. E. ―*Pillared graphene: a new 3-D network nanostructure for enhanced hydrogen storage*‖. Nano letters, 8(10), **(2008).** 3166-3170.
3. Hall, Christopher. "*Polymer Materials and their Technology*." Polymer Materials. Macmillan Education UK, **1981**. 141-183.
4. Katnam, K. B., L. F. M. Da Silva, and T. M. Young. "*Bonded repair of composite aircraft structures: A review of scientific challenges and opportunities*." Progress in Aerospace Sciences 61 **(2013**): 26-42.
5. Naik, N. K., and P. S. Shembekar. "*Elastic behavior of woven fabric composites: I—Lamina analysis*." Journal of composite materials 26.15 **(1992).** 2196-2225.
6. Yu, Dingshan, and Liming Dai. "*Self-assembled graphene/carbon nanotube hybrid films for supercapacitors*." The Journal of Physical Chemistry Letters 1.2 **(2009)**: 467-470.
7. Miracle, D. B. "*Metal matrix composites–from science to technological significance*." Composites science and technology 65.15 **(2005):** 2526-2540.
8. Mohan, N. S., S. M. Kulkarni, and A. Ramachandra. "*Delamination analysis in drilling process of glass fiber reinforced plastic (GFRP) composite materials*." Journal of Materials Processing Technology 186.1 **(2007):** 265-271.

9. Yang, WH P., and Y. S. Tarng. "*Design optimization of cutting parameters for turning operations based on the Taguchi method*." Journal of materials processing technology 84.1 **(1998):** 122-129.
10. Cohen, Charles J.,et al. "*Behavior recognition architecture for surveillance applications*." Applied Imagery Pattern Recognition Workshop, 2008. AIPR'08. 37th IEEE. IEEE, **2008.**
11. Kuo, Tsai-C., Samuel H. Huang, and Hong-C. Zhang. "*Design for manufacture and design for ‗X': concepts, applications, and perspectives*." Computers & industrial engineering 41.3 **(2001):** 241-260.
12. Asiltürk I, Akkuş H. ―*Determining the effect of cutting parameters on surface roughness in hard turning using the Taguchi method. Measurement*‖. Nov 30;44(9) **2011**:1697-704.
13. Bianco, Alberto. "*All in the graphene family–a recommended nomenclature for two-dimensional carbon materials*." **(2013):** 1-6.
14. Kuilla, T., Bhadra, S., Yao, D., Kim, N. H., Bose, S., & Lee, J. H. ―*Recent advances in graphene based polymer composites*‖. Progress in polymer science, 35(11**), (2010).** 1350-1375.
15. Lavoisier, A.Laurent. ―*Elements of chemistry, in a new systematic order: containing all the modern discoveries. Courier Corporation*‖. **1965.**
16. Bery, Vikas. "*Impermeability of graphene and its applications*." Carbon 62 **(2013):** 1-10.
17. Pierson, Hugh O. ―*Handbook of carbon, graphite, diamonds and fullerenes: processing, properties and applications. William Andrew*‖, **2012.**
18. Gómez-Navarro, C., Meyer, J. C., Sundaram, R. S., Chuvilin, A., Kurasch, S., Burghard, M., & Kaiser, U. ―*Atomic structure of reduced graphene oxide*. Nano letters‖. 10(4), **(2010).** 1144-1148.

19. Sahithi, K., Swetha, M., Ramasamy, K., Srinivasan, N., & Selvamurugan, N. ―*Polymeric composites containing carbon nanotubes for bone tissue engineering*‖. International journal of biological macromolecules, 46(3), **(2010):** 281-283.
20. Sheng, Zhen-Huan. "*Catalyst-free synthesis of nitrogen-doped graphene via thermal annealing graphite oxide with melamine and its excellent electrocatalysis*." ACS nano 5.6 **(2011):** 4350-4358.
21. Thompson, T. J. U., Marie Gauthier, and Meez Islam. "*The application of a new method of Fourier Transform Infrared Spectroscopy to the analysis of burned bone*." Journal of Archaeological Science 36.3 **(2009):** 910-914.
22. Coates, John. "*Interpretation of infrared spectra, a practical approach*." Encyclopedia of analytical chemistry **(2000).**
23. Goldstein, Joseph. Scanning electron microscopy and X-ray microanalysis: ―*A text for biologists, materials scientists, and geologists*‖. Springer Science & Business Media, **2012.**
24. Vogel, S. F. "*Pyrolytic graphite in the design of a compact inert heater of a lanthanum hexaboride cathode*." Review of Scientific Instruments 41.4 **(1970):** 585-587.
25. Pradhan, Subhashree. ―*Production and characterization of Activated Carbon produced from a suitable Industrial sludge*‖. Diss. **2011.**
26. Soper, A. K. "*The radial distribution functions of water and ice from 220 to 673 K and at pressures up to 400 MPa.*" Chemical Physics 258.2 **(2000):** 121-137.
27. Gutowski, Timothy, Jeffrey Dahmus, and Alex Thiriez. "*Electrical energy requirements for manufacturing processes.*" 13th CIRP international conference on life cycle engineering. Vol. 31. **2006.**

28. García-Nieto, Paulino José, et al. "*A new predictive model based on the PSO-optimized support vector machine approach for predicting the milling tool wear from milling runs experimental data*." The International Journal of Advanced Manufacturing Technology 86.1-4 **(2016):** 769-780.

29. Singh, Hardeep, G.Akhyar, and M. P. Garg. "*Effect of cutting parameters on MRR and surface roughness in turning EN-8.*" Current Trends in Engineering Research 1.1 **(2011).**

30. Panneerselvam, Hari, Vasudevan, K. Pradeep, and P. Asokan. "*Optimization of end milling parameters for glass fiber reinforced plastic (GFRP) using grey relational analysis.*" Procedia Engineering 38 **(2012):** 3962-3968.

31. Ghhani J. A, Zhang, Julie Z., Joseph C. Chen, and E. Daniel Kirby. "*Surface roughness optimization in an end-milling operation using the Taguchi design method*." Journal of materials processing technology 184.1 **(2007):** 233-239.

32. Nayak, Shreemoy Kumar, et al. "*Multi-objective optimization of machining parameters during dry turning of AISI 304 austenitic stainless steel using grey relational analysis."* Procedia Materials Science **6 (2014):** 701-708.

33. Chen, Ji, et al. "*An improved Hummers method for eco-friendly synthesis of graphene oxide.*" Carbon 64 **(2013):** 225-229.

34. Unal, Resit, and Edwin B. Dean. "*Taguchi approach to design optimization for quality and cost: an overview*." **(1991).**